Reaction Intermediates in the Selective Catalytic Reduction of NO$_x$ over Fe/ZSM-5

Hai-Ying Chen, Timur Voskoboinikov, and Wolfgang M. H. Sachtler

V. N. Ipatieff Laboratory, Center for Catalysis and Surface Science, Department of Chemistry, 2137 Sheridan Road,
Northwestern University, Evanston, Illinois 60208
E-mail: wmhs@nwu.edu

For the selective catalytic reduction of NO$_x$ with alkanes to N$_2$ over Fe/ZSM-5 catalysts, prepared by sublimation, we had previously shown that NO is oxidized over Fe–oxo ions to NO$_2$ which forms chemisorbed NO$_y$ complexes. Subsequent reaction of the NO$_y$ groups with alkanes results in N-containing deposits that react with different adsorbed NO$_2$ molecules to form N$_2$. At low temperature, the reactivity of *n*-butane exceeds that of *i*-butane. Quantitative evaluation of the reaction kinetics for the deposits from not only propane and butanes but also adsorbed model compounds, including ammonia, amines, nitriles, and isocyanates, provide information on the reaction steps on the catalyst surface. Reaction of NO$_2$ with the catalyst deposit follows Langmuir–Hinshelwood kinetics. The primary intermediates which contain N atoms at a high valence state have to be transformed into deposits containing amino groups. Nitrogen–nitrogen bonds are formed when these groups react with adsorbed NO$_2$. The chemical reactions, transforming the primary intermediate into a deposit containing N atoms in a low oxidation state, are easy if an H atom is available in the α position with respect to the NO$_2$ group; the absence of such H atoms in the primary product from *i*-butane is the cause for its lower reactivity. ©1999 Academic Press

Key Words: DeNO$_x$ catalysts; SCR of NO$_x$; Fe/ZSM-5; chemical vapor deposition; transformation of adsorbed nitro compounds to amines.

1. INTRODUCTION

Numerous catalysts have been reported to catalyze the selective catalytic reduction (SCR) of NO$_x$ by hydrocarbons in the presence of excess oxygen (1–6). However, most of these catalysts lose much of their activity in the presence of water vapor. Overexchanged Fe/ZSM-5 catalysts have been found to be highly active and remarkably stable for the SCR reaction in the presence of H$_2$O (7–11). In these studies, *i*-butane was used as a reductant. Recently, it was found that the catalytic performance of the Fe/ZSM-5 catalysts that are prepared by a sublimation method strongly depends on the nature of hydrocarbons in a nontrivial manner (12). Methane is inactive; propene is less active than alkanes such as propane, and the activity ranking of the alkanes depends

on the temperature: the maximum N$_2$ yield is higher for *i*-butane than for propane, but *i*-butane reaches this maximum at a higher temperature. Below the maximum temperature, propane shows higher activity than *i*-butane. In the same paper, we also established that an active N-containing deposit is formed on the Fe/ZSM-5 catalyst by the reaction of the hydrocarbon with adsorbed nitro/nitrate groups, further to be called NO$_y$ complexes. Upon subsequently exposing the deposit to NO$_2$ (or NO + O$_2$), large amounts of N$_2$ are formed. Isotopic labeling shows that one N atom in every N$_2$ molecule comes from the deposit and the other from NO$_2$. However, unraveling the nature of these active deposits is still a challenging task.

The role of N-containing surface species in the SCR of NO$_x$ by hydrocarbons has recently been recognized. Several reaction mechanisms involving different reaction intermediates have been proposed. On the basis of the appearance of an IR band at 2234 cm^{-1} upon exposing Cu/alumina catalysts to a simulated gas mixture, Ukisu *et al.* (13, 14) proposed isocyanates to be the intermediates. Although their IR band assignment was adopted by Bell *et al.* (15) for Cu/ZSM-5 catalysts in the SCR of NO$_x$ with propene, Hayes *et al.* (16, 17) argue that these bands are better assigned to nitriles rather than isocyanates because the complex appears to be stable against water. Their results also suggest that the nitriles are not active enough to be true reaction intermediates. Instead, they propose that organic nitro compounds will be intermediates; these could be decomposed to nitrogen via a diazo intermediate. The group of Kung (18, 19) found that N-containing surface intermediates are formed on Cu/ZrO$_2$ and Cu/ZSM-5 catalysts when adsorbed NO$_2$ reacts with an adsorbed hydrocarbon; N$_2$ is produced when these intermediates react with NO. On the basis of their IR results, these authors consider CN and NCO as potentially active groups. Radtke *et al.* (20–22) detected HCN, HNCO, and NH$_3$ in the gas phase by FTIR during the SCR of NO$_x$ by olefins over Cu/ZSM-5 and Cu/γ-Al$_2$O$_3$. In a later paper (23), they suggest that nitriles or oximes could be reaction intermediates. The formation of ammonia during SCR of NO$_x$ with propane over

Cu/ZSM-5 was also proposed by Poignant et al. (24, 25) on the basis of their FTIR results. They attributed the NH_3 formation to the hydrolysis of isocyanate groups. Aylor et al. (26, 27) argue that nitriles, not isocyanates, are reaction intermediates in the SCR of NO_x by CH_4 over Co/ZSM-5. In summary, the presence of nitriles and/or isocyanates, either as intermediates or as by-products in the SCR of NO_x with hydrocarbons, appears well documented.

Obviously, these compounds cannot be formed in one step. Misono et al. (28–30) proposed that organic nitro and nitrite compounds could be the initial products, which might react further with O_2 or NO_x to N_2. However, no details have been given how the latter reactions could occur. Li et al. (31) proposed that nitromethane may be an initial product in the SCR of NO_x by CH_4 over Co/ZSM-5. The involvement of nitromethane was further studied by the groups of Cant (32, 33) and Hall (34). Referring to the work of Blower and Smith (35), they propose reaction schemes in which the rearrangement of nitromethane is emphasized. The products with nitrogen at low oxidation state were considered to be the active groups that further react with NO_x or O_2 to form N_2. With a Fe–silicalite catalyst and propene as the reductant, Yogo et al. (36) found that an N-containing organic intermediate can be formed on the catalyst when adsorbed C_3H_6 and NO interact; upon exposure of this deposit-covered catalyst to NO (or NO_2), nitrogen is produced. Using a two-step experiment, Guyon et al. (37) also found an active N-containing deposit on Cu/ZSM-5 which reacts with NO_2 or $NO + O_2$ to form N_2. However, in these papers, no attempt is made to identify the nature of the active deposits.

Previous results in this lab suggest that organic nitroso or nitro compounds may be the initial products in the SCR of NO_x with alkanes over Cu/ZSM-5 (38–40). In the case of propane, the initial product, 2-nitosopropane, is assumed to spontaneously isomerize to acetone oxime. Indeed, adsorbed acetone oxime shows high reactivity toward NO, yielding N_2 and N_2O. Isotopically mixed molecules $^{14}N^{15}N$ and $^{14}N^{15}NO$ were found to be the main products when ^{15}NO reacts with ^{14}N-labeled acetone oxime.

Since the formation of organic nitroso and nitro compounds and their isomerization depend on the nature of the hydrocarbon, it is expected that different hydrocarbons will result in different intermediates. In the present work, N-containing deposits were laid down on Fe/ZSM-5 following the same procedure as reported in our previous paper (12), but with three different alkanes: C_3H_8, n-C_4H_{10}, and i-C_4H_{10}. Their reactivity toward $NO + O_2$ was measured in a recirculation system. Also, some N-containing model compounds were introduced onto the Fe/ZSM-5 catalyst, and their reactivity toward $NO + O_2$ was compared with that of the deposits. FTIR spectra under similar reaction conditions were registered to identify the active groups.

2. EXPERIMENTAL

2.1. Catalyst Preparation

The parent ZSM-5 zeolite, obtained from UOP (lot#13923, Si/Al = 14.2, Na/Al = 0.67), was first calcined in an O_2 flow at 550°C for 4 h to remove any residual hydrocarbon templet. Na/ZSM-5 was prepared by back exchanging the calcined sample with dilute $NaNO_3$ solution at pH 10 three times. Virtually no Brønsted acid sites are detected by FTIR; H/ZSM-5 was prepared by triple exchange of the calcined sample with a dilute $NH_4 \cdot NO_3$ solution, followed by calcination in an O_2 flow at 550°C for 4 h; Fe/ZSM-5 was prepared by chemical vapor deposition, i.e., subliming $FeCl_3$ onto H/ZSM-5 as described in previous papers (9–11). The Fe/ZSM-5 sample used in this work is the same as the one used in our previous work (12).

2.2. Reactivity of Adsorbate

A recirculating manifold equipped with a Dycor Quadrupole Gas Analyzer was used to determine the reactivity of adsorbates toward $NO + O_2$. The volume of the circulation loop is 145 ml when the reactor is bypassed. It becomes 166 ml when the reactor is opened. A magnetically driven gas circulation pump was installed inside the loop to mix the reactant gases, and also to make the flow of gases through the catalyst. The gas flow rate is about 80 ml/min at a pressure of 100 Torr (1 Torr = 133.32 Pa). A 0.400-g Fe/ZSM-5 (340 μmol of Fe) catalyst was charged in a Pyrex reactor which was attached to this system. Prior to the experiment, the sample was pretreated by being calcined at 500°C in an O_2 flow of 100 ml/min for 1 h and cooled to 200°C under the same flow. With the catalyst being held at this temperature, some of the steps (1)–(3) were carried out; before each of them, the entire circulation loop was evacuated (background pressure, 10^{-3} Torr) for 0.5 h.

(1) A gas mixture of 10 Torr ^{14}NO (~78 μmol), 10 Torr Ar (~78 μmol), and 80 Torr O_2 (~624 μmol) was admitted to the circulation loop with the reactor being bypassed. After being mixed for 1 h, it was circulated over the catalyst for 45 min. As shown in our previous paper (12), this procedure results in the formation of NO_y adsorption complexes on the catalyst.

(2) Same as (1), but n-C_4H_{10} (or C_3H_8, i-C_4H_{10}) was used instead of NO to react with the adsorption complex(es) formed in step (1). As shown previously (12), a nitrogen-containing deposit is formed in this step.

(2′) If deposition of a nitrogen-containing model compound was desired, steps (1) and (2) were replaced by the following: 2 Torr $^{14}NH_3$ or ^{14}N-containing organic compound was mixed with 10 Torr Ar (~78 μmol) and 80 Torr O_2 (~624 μmol) in the circulation loop with the reactor being bypassed. The ^{14}N-labeled organic compounds used were $C_2H_5NH_2$, CH_3CN, $CH_2{=}C(CH_3){-}CN$, C_2H_5NCO, or

$(CH_3)_2CHNO_2$. (In the case of $(CH_3)_2CHNO_2$, 10 Torr sample was used because of its decomposition. See below.) After the sample was mixed for 1 h, the gas was circulated over the catalyst for 45 min. The amount of the model compound was dosed so that approximately the same number of N atoms were present on the catalysts as in the deposit laid down by the reaction of NO$_y$ with hydrocarbon.

(3) A gas mixture of 10 Torr ^{15}NO ($\sim$78 μmol), 10 Torr Ar ($\sim$78 μmol), and 80 Torr O$_2$ ($\sim$624 μmol) was admitted to the circulation loop with the reactor being bypassed. After being mixed for 1 h, almost all of the ^{15}NO was found converted to ^{15}NO$_2$. This mixture was allowed to circulate over the catalyst for 45 min, while the gas phase composition was monitored every 30 s by a mass spectrometer. For kinetic measurements the initial partial pressure of ^{15}NO was varied from 5 to 26 Torr, while the initial partial pressure of O$_2$ was changed to maintain a total pressure of 100 Torr. For the MS analysis Ar was added as an internal standard. Data processing and curve fitting was done by SigmaPlot.

2.3. FTIR Measurements

FTIR spectra were collected on a Nicolet 680SX FTIR spectrometer equipped with a liquid N$_2$-cooled MCT detector. The sample was pressed into a self-supporting wafer of 8–10 mg/cm^2. The wafer was loaded into a quartz cell sealed with NaCl windows. The cell is connected to a gas manifold. Prior to any experiment, the sample was calcined *in situ* at 500°C for 1 h in an O$_2$/He (3%) flow of 100 ml and cooled to 200°C. NO$_y$ complexes were then formed on the catalyst by flowing a gas consisting of NO (0.5%), O$_2$ (3%), and He at 100 ml/min through the cell for 30 min, followed by 30 min of purging with 3% O$_2$. Subsequently, n-C$_4$H$_{10}$ (0.2%) + O$_2$ (3%) + He at 100 ml/min was flowed through the cell for 30 min to lay down a deposit on the catalyst. After the mixture was purged with O$_2$ (3%) for another 30 min, NO (0.5%) + O$_2$ (3%) was again introduced to the cell and the spectrum was recorded as a function of time. To check the reactivity of the model compounds, their vapor was first introduced into the cell by an O$_2$/He (3%) flow for about 30 min. This was also followed by purge with O$_2$/He (3%). All spectra were registered at 200°C unless specified otherwise; 50 scans were accumulated with a spectral resolution of 1 cm^{-1}. The gas inside the cell, immediately after scanning of the sample, was used as the spectroscopic background. The spectrum of the calcined sample is used as a reference; it is subtracted from the spectrum measured under flow conditions.

2.4. XPS Measurements

The nitrogen valence state of the deposit on Fe/ZSM-5 was analyzed by XPS. These measurements were performed with a VG ESCA Lab spectrometer using Al$K\alpha$ excitation ($h\nu = 1486.3$ eV). During the analysis, the pressure in the analyzer chamber was maintained below 5×10^{-9} Torr.

A powdered sample of Fe/ZSM-5 was pressed into a self-supported disc $\sim$5 mm in diameter and stuck to the sample holder by colloid silver. Deposits were created in an *in situ* high-pressure cell by exposing Fe/ZSM-5 to a flow of i-C$_4$H$_{10}$ + NO$_2$ at 320°C for 1 h. The Si2p line (BE = 103.6 eV) of the zeolite support was used as an internal standard. The position of the N1s peak was determined within an accuracy of 0.1 eV.

3. RESULTS

Previously, we had shown (12) that the isotopically mixed molecule ^{15}N^{14}N was the predominant dinitrogen that was produced when ^{15}NO + O$_2$ interacted with a deposit that had been laid down by the reaction of ^{14}NO$_y$ with i-C$_4$H$_{10}$. The rate by which this ^{15}N^{14}N was formed fits an exponential function ($f = A(1 - e^{-k't})$) well (see Fig. 16 in Ref. (12)). The same pattern was found to hold for deposits formed from C$_3$H$_8$ or n-C$_4$H$_{10}$ and also for some model compounds. In Fig. 1, the experimental data (dots) and the fitting curve (solid line) are shown for the reaction where a deposit, laid down by exposing ^{14}NO$_y$ to n-C$_4$H$_{10}$, was subsequently exposed to ^{15}NO + O$_2$. This result was found quite reproducible if the partial pressure of each component was kept at the same initial value in each step. This also holds for the factor k', which, however, strongly depends on the hydrocarbon used for the formation of the deposit. A higher k' value means that the concentration of ^{15}N^{14}N inside the circulation loop increases faster, i.e., the deposit shows higher reactivity toward NO$_2$. In the top section of Table 1, the k'
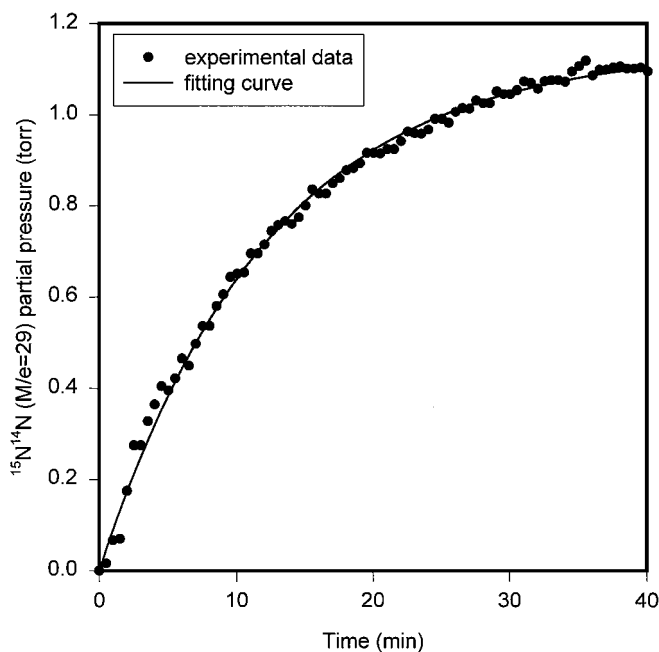

FIG. 1. ^{15}N^{14}N partial pressure as a function of time upon exposing a ^{14}N deposit, formed by reaction of NO$_y$ with n-C$_4$H$_{10}$, to ^{15}NO + O$_2$.

TABLE 1

k' Values and $^{15}N_2/^{15}N^{14}N$ Ratio for Different Deposits
and Model Compounds

Deposits formed by	k' (min^{-1})	$^{15}N_2/^{15}N^{14}N$
$NO_y + C_3H_8$	0.085	0.05
$NO_y + n\text{-}C_4H_{10}$	0.083	0.15
$NO_y + i\text{-}C_4H_{10}$	0.073	0.15
NH_3	0.163	0
$C_2H_5NH_2$	0.175	0
CH_3CN	0.066	0
$CH_2=C(CH_3)-CN$	0.035	0.27
C_2H_5NCO	0.099	0.33
$(CH_3)_2CHNO_2$	0.045	0.15

values are listed for deposits formed with different alkanes. It shows that equal k' values for the deposits formed with C_3H_8 and $n\text{-}C_4H_{10}$, but a lower value formed for the deposit from $i\text{-}C_4H_{10}$. In the same table, the ratio of $^{15}N_2/^{15}N^{14}N$ after 40 min of reaction is given. Among the deposits from alkanes, it has its lowest values for that produced from C_3H_8.

Since k' relates to the reactivity of the deposits toward $NO + O_2$, it enables us to also compare the reactivity of these deposits with that of some model compounds which we laid down on the catalyst and exposed to $NO + O_2$ at the same conditions. In the bottom section of Table 1, these k' values and $^{15}N_2/^{15}N^{14}N$ ratios are listed.

The data show that over Fe/ZSM-5 the highest reactivity toward NO_2 is found with NH_3 and $C_2H_5NH_2$. However, it should be mentioned that $C_2H_5NH_2$ reacts readily with NO_2, even at room temperature and in the absence of an Fe/ZSM-5 catalyst. In a blank test, we observed the formation of $^{15}N^{14}N$ when $^{15}NO_2$ was circulated through the loop, holding a small amount of $C_2H_5^{14}NH_2$. This is consistent with well-known organic chemistry that says primary amines react readily with NO_2, forming N_2 via a diazo (or diazonium) compound (41, 42). For these model compounds, $^{15}N^{14}N$ is the only dinitrogen product.

Adsorbed CH_3CN also reacts with NO_2 over Fe/ZSM-5 forming $^{15}N^{14}N$ as the only N_2 product; however, its k' value is lower. Interestingly, methacrylonitrile, $CH_2=C(CH_3)-CN$, though having the same nitrile group, has a still lower k' value, and in its interaction with $^{15}NO_2$ significant amounts of $^{15}N_2$ are formed. Ethyl isocyanate, C_2H_5NCO, on Fe/ZSM-5, which is unstable at 200°C (see FTIR results below), is highly reactive toward NO_2, as demonstrated by its larger k' value. Also for this molecule, the $^{15}N_2/^{15}N^{14}N$ ratio is rather high.

2-Nitropropane, $(CH_3)_2CHNO_2$, decomposes over Fe/ZSM-5 at 200°C, changing the color of the catalyst from light yellow to gray. Interestingly, a deposit is also formed in this decomposition; it contains nitrogen and reacts with $^{15}NO_2$, producing $^{15}N^{14}N$, though with a lower k' value. Also, some $^{15}N_2$ is formed in this process.

The k' values in Table 1 were obtained by using the same NO_2 initial partial pressure in each run. Actually, k' depends on P_{NO_2} as shown in Fig. 2. The experimental data (dots) scatter around a curve (solid line) fitting a Langmuirian function $k' = k \times [b \times P_{NO_2}/(1 + b \times P_{NO_2})]$.

The FTIR spectrum of the deposit formed on Fe/ZSM-5 by reaction of NO_y with $n\text{-}C_4H_{10}$ is shown in Fig. 3a. It has broad bands in the 1700- to 1300-cm^{-1} region, with a few maxima at 1670, 1573, 1437, 1377, and 1357 cm^{-1}, indicating that the deposit is rather complicated. In addition, there is a band at 1876 cm^{-1}, which we have assigned to mononitrosyl ligands of iron ions (12). A negative band at 3665 cm^{-1} is also present. It is located between the bands of SiOH (3710 cm^{-1}) and Brønsted acid sites (3605 cm^{-1}). This band is tentatively assigned to OH groups attached to iron ions, as expected for the binuclear ion $[HO-Fe-O-Fe-OH]^{2+}$ that we proposed previously (9–11). Its negative intensity suggests that the deposit covers iron sites, displacing their OH ligands. Upon exposure of the sample covered with the deposit to an $NO + O_2$ flow, the intensity of the bands characteristic for the deposit decreases with time; meanwhile, new bands appear for the NO^+ group on Brønsted sites (2311 cm^{-1}), the mononitrosyl ligand (1877 cm^{-1}), the nitro group (1625 cm^{-1}), and the nitrate ions (1570 cm^{-1}), as shown in Figs. 3b–3e. The assignment for these bands has been discussed before (12). During this reaction, the bands at 1670, 1573, and 1377 cm^{-1} decline rather rapidly during the first few minutes, suggesting that they have to be assigned to active groups. In contrast, the bands at 1437 and 1357 cm^{-1} hardly change; they are assigned to carbonate
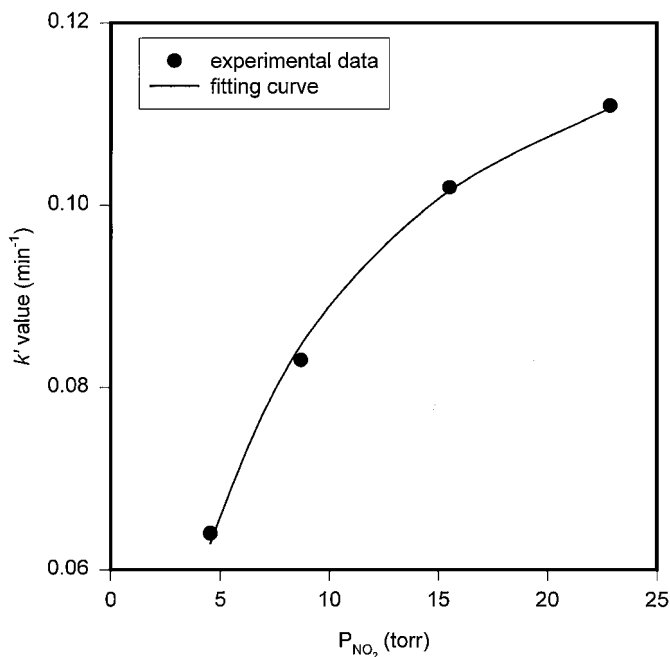

FIG. 2. Dependence of the rate constant k' on the partial pressure P_{NO_2}.
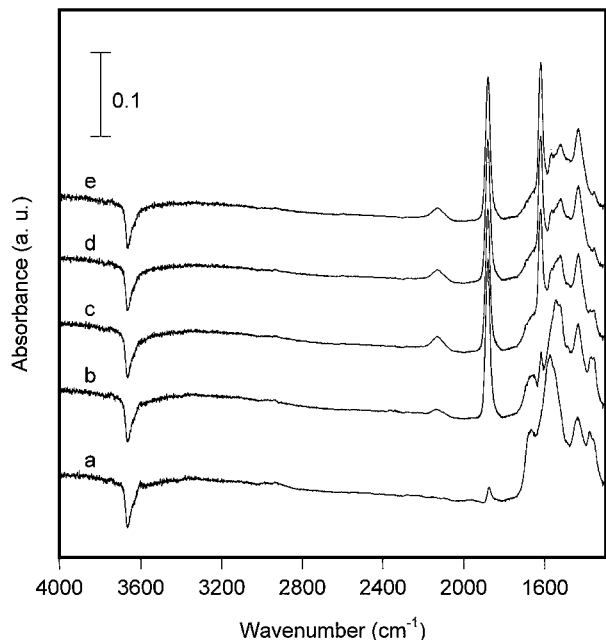
FIG. 3. FTIR spectra taken at 200°C as a function of time when an N-containing deposit, formed by reaction of NO$_y$ with n-C$_4$H$_{10}$, was subsequently exposed to a flow of NO + O$_2$ for (a)–(e) 0, 2, 5, 15, or 30 min.

groups (12). After 30 min, another band at 1522 cm^{-1} became evident; it could be assigned to a carboxylate group (43).

The FTIR spectrum of acetonitrile adsorbed on Fe/ZSM-5 is shown in Fig. 4a. Bands at 2999 and 2934 cm^{-1} and 1371

and 1357 cm^{-1} can be assigned to C–H stretching and deformation frequencies, respectively. A doublet at 2314 and 2285 cm^{-1} is due to the C≡N stretching vibration. Negative bands at 3665 and 3605 cm^{-1} suggest that acetonitrile was adsorbed both on iron and Brønsted acid sites. In the same spectrum, a band at 1666 cm^{-1} with a shoulder at 1693 cm^{-1} and a broad band centering at 1570 cm^{-1} are present. They can be assigned to amide(I) and amide(II) bands, respectively (see below). Correspondingly, weak bands are visible at 3465 and 3375 cm^{-1}, which could be assigned to the N–H stretching vibrations of an amino group (43). Upon exposure to an NO + O$_2$ flow, the bands attributed to amide groups declined rather quickly and almost vanish after 5 min. The intensity of the C≡N bands decreases with time in concert with an increase of the intensity of the mononitrosyl (1877 cm^{-1}) and the nitro/nitrate groups (1625 and 1570 cm^{-1}). This suggests that these species are all adsorbed on the same iron sites. During this reaction, carbonate (bands at 1437 and 1357 cm^{-1}) and carboxylate ions (1522 cm^{-1}) are formed.

Hydrolysis of acetonitrile is a possible cause for the appearance of an amide group on Fe/ZSM-5:

$$CH_3CN + H_2O \rightarrow CH_3-C(O)-NH_2. \qquad [1]$$
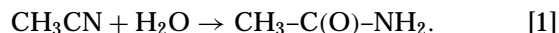
This reaction is well known to be catalyzed by protons. Figure 5a shows the FTIR spectrum of acetonitrile adsorbed on H/ZSM-5. Besides the bands assigned to acetonitrile (C–H stretching vibration at 2935 and 2999 cm^{-1}, C–H
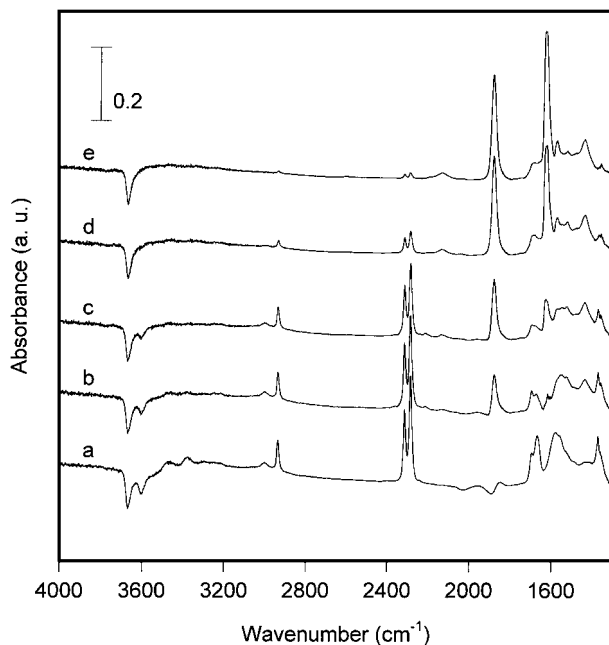

FIG. 4. FTIR spectra taken at 200°C as a function of time when a CH$_3$CN adsorbed Fe/ZSM-5 sample was exposed to NO + O$_2$ flow for (a)–(e) 0, 2, 5, 15, and 30 min.
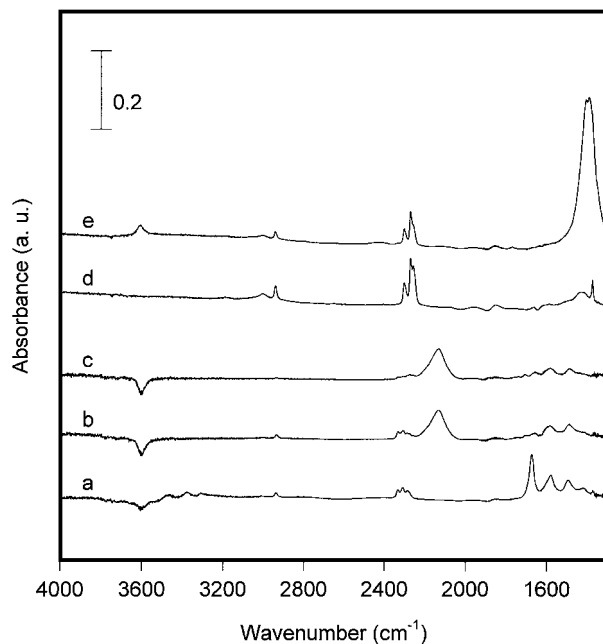

FIG. 5. FTIR spectra taken at 200°C. (a)–(c) A CH$_3$CN adsorbed H/ZSM-5 sample was exposed to NO + O$_2$ flow for 0, 5, and 30 min, respectively; (d) and (e) a CH$_3$CN adsorbed Na/ZSM-5 sample was exposed to NO + O$_2$ flow for 0 or 30 min.

deformation vibration at 1370 cm^{-1}, and C≡N stretching vibration at 2332, 2308, and 2285 cm^{-1}), additional intensive bands appear at 1671, 1578, and 1491 cm^{-1}. Weak bands at 3462, 3377, and 3308 cm^{-1} are also visible. It is reasonable to assign them to an amide group. This group is very reactive toward NO + O$_2$ as shown in Fig. 5b; all these bands have vanished afer 5 min. By using the circulation system, we could confirm that this reaction leads exclusively to the formation of isotopically mixed dinitrogen, ^{15}N^{14}N. In the absence of protons, Reaction [1] hardly occurs, as shown in Fig. 5d. The FTIR spectrum of CH$_3$CN adsorbed on Na/ZSM-5 only shows the acetonitrile bands. Upon exposure to NO + O$_2$, almost no change was observed for these bands; see Fig. 5e. This finding is consistent with the result obtained by using the circulation system; i.e., no gas phase product was observed upon circulating NO$_2$ over CH$_3$CN-adsorbed Na/ZSM-5. In contrast, NH$_3$ shows the same reactivity toward NO + O$_2$ when adsorbed either on Fe/ZSM-5 or on Na/ZSM-5 as was shown in a separate experiment. Therefore, it appears that it is the hydrolysis product, not the nitrile itself, that reacts with NO$_2$.

The FTIR spectrum of an Fe/ZSM-5 sample covered with adsorbed methacrylonitrile is shown in Fig. 6a. Because of its conjugated structure, an intensive band at 2255 cm^{-1} is observed for the C≡N stretching vibration; weak bands centering at 1670 and 1573 cm^{-1} are also visible. This adsorption complex shows low reactivity toward NO + O$_2$, as can be seen from the spectra in Figs. 6b–6d. After exposure to flowing NO + O$_2$ for 60 min, a band at 2255 cm^{-1} is still
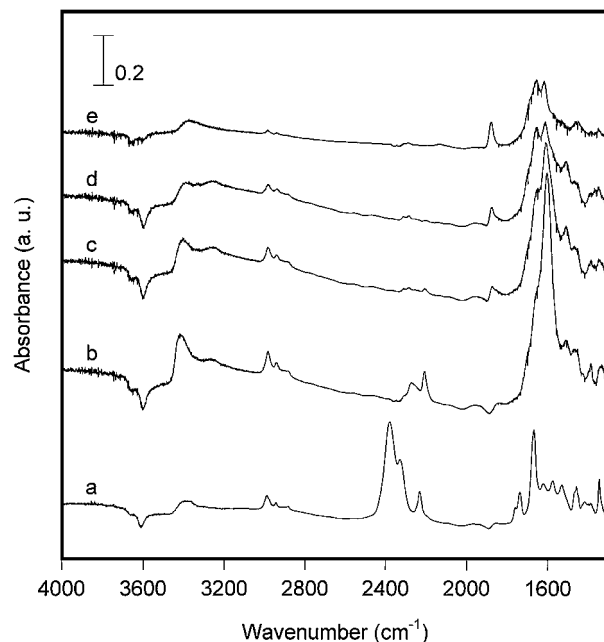

FIG. 7. FTIR spectra: (a) taken at RT after Fe/ZSM-5 being exposed to C$_2$H$_5$NCO at RT in He flow; (b) taken at 200°C after Fe/ZSM-5 being exposed to C$_2$H$_5$NCO at 200°C in O$_2$/He(3%) flow; (c)–(e) following (b), the sample was further exposed to NO + O$_2$ flow for 2, 5, or 30 min.

FIG. 6. FTIR spectra taken at 200°C as a function of time when a CH$_2$=C(CH$_3$)–CN adsorbed Fe/ZSM-5 sample was exposed to NO + O$_2$ flow for (a)–(e) 0, 2, 5, 20, or 60 min.

present. The bands at 1670 and 1573 cm^{-1} again declined faster, revealing some reaction with NO$_2$.

The isocyanate C$_2$H$_5$NCO is not stable on Fe/ZSM-5; see Figs. 7a and 7b. Spectrum (a) is recorded at room temperature (RT) under a helium atmosphere, while spectrum (b) is recorded at 200°C under an O$_2$ (3%) flow. Broad bands at 3412 and 3260 cm^{-1} in spectrum (b) indicate that NH$_3$, amine, or/and amide groups might be decomposition products. An intensive band at 1606 cm^{-1} indicates the formation of a C=C double bond. It is possible that an oligomer is formed on the catalyst when C$_2$H$_5$NCO decomposes. Bands at 2273 and 2209 cm^{-1} can be assigned to N=C=O groups adsorbed on Fe sites (44, 45). They vanish after exposure to NO + O$_2$ for 5 min (Fig. 7c). Also, the intensity of bands at 3412 and 1606 cm^{-1} decreases dramatically during the first 5 min.

Organic nitro compounds are well known to be thermally unstable (46). Decomposition of 2-nitropropane over Fe/ZSM-5 at 200°C forms a deposit on the catalyst, as shown in Fig. 8a. Bands in the 1700- to 1300-cm^{-1} region are similar to those in Fig. 3a. In addition, bands in the C≡N stretching vibration region, at 2314, 2286, and 2257 cm^{-1}, are obvious. Bands at 2314 and 2286 cm^{-1} can be assigned to the C≡N group from a saturated aliphatic nitrile, as both the wavenumber and the relative intensity are exactly the same as those in Fig. 4a. A band at 2257 cm^{-1} has the same wavenumber as was observed in Fig. 6a; it can be assigned to the C≡N stretching virbation of an unsaturated aliphatic
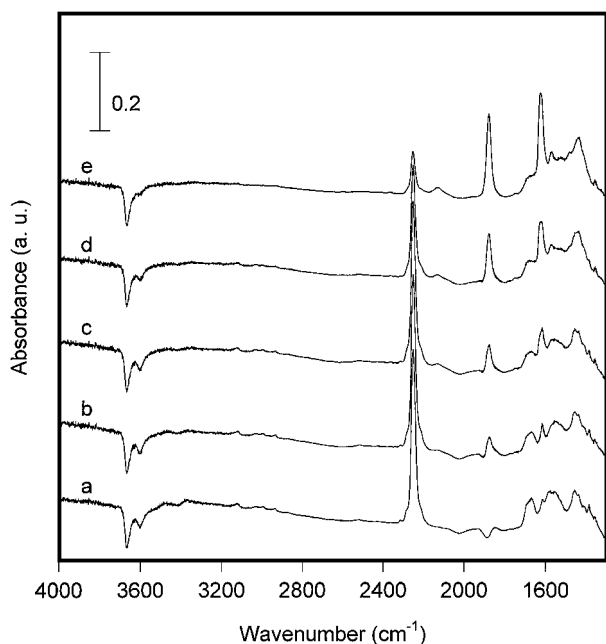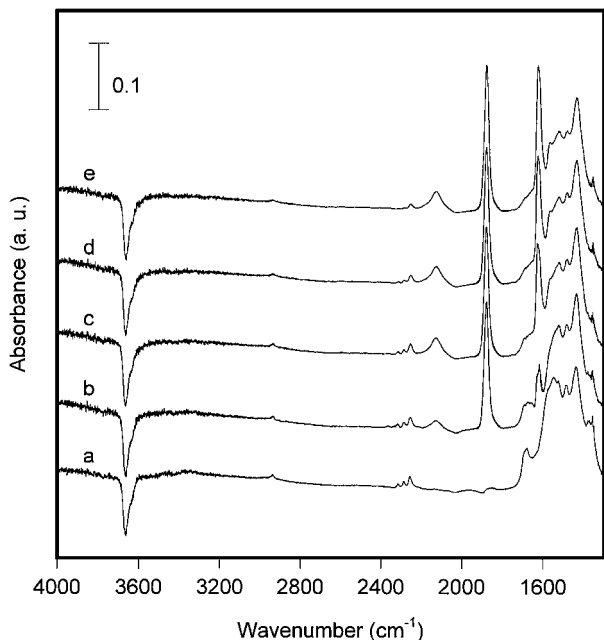
FIG. 8. FTIR spectra taken at 200°C: (a) after the Fe/ZSM-5 sample being exposed to $(CH_3)_2CH(NO_2)$; (b)–(e) following (a), the sample was further exposed to $NO + O_2$ flow for 2, 5, 15, or 30 min.

nitrile. Upon exposure to $NO + O_2$, the intensity of the bands in the 1700- to 1300-cm^{-1} region decreases to some extent, especially the maxima at 1680 and 1573 cm^{-1}. Also, the intensity of the bands at 2314 and 2286 cm^{-1} decreases with time, but the band at 2257 cm^{-1} declines more slowly.

4. DISCUSSION

The results of this work and our previous studies with labeled nitrogen show that the main path for the formation of dinitrogen is via the reaction of NO$_2$ with an N-containing deposit, $C_aH_bO_c{}^{14}N$, on the catalyst:

$$^{15}NO_2 + C_aH_bO_c{}^{14}N$$
$$\rightarrow {}^{15}N^{14}N + C_{a'}H_{b'}O_{c'} + yCO_x + zH_2O. \quad [2]$$
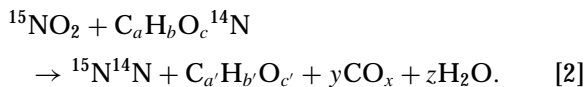
Here, we only consider the productive reaction, i.e., the reaction that leads to N$_2$ formation. Side reactions, such as the reduction of NO$_2$ to NO by hydrocarbons, are ignored. As shown in Ref. (12), compared with NO$_2$, NO itself reacts very slowly with a N-containing deposit forming N$_2$. Instead, under the conditions applied in this study, it will be oxidized by O$_2$ back to NO$_2$.

With Reaction [2], we can write, for the rate of $^{15}N^{14}N$ formation,

$$r = \partial[^{15}N^{14}N]/\partial t = k \times P_{NO_2}^m \times [C_aH_bO_c{}^{14}N]^n. \quad [3]$$

For the circulation experiment, 0.4 g of catalyst, i.e., 340 μmol of Fe, was used. The amount of deposit was usu-

ally controlled to be about 10–15 μmol (based on N). The amount of NO$_2$ admitted to the loop was set at 78 μmol in most cases. So, we can ignore the change of partial pressure of NO$_2$ during the reaction and simplify to $k' = k \times P_{NO_2}^m \approx$ constant. For the surface concentration of $C_aH_bO_c{}^{14}N$ we have $[C_aH_bO_c{}^{14}N] = C_0 - [^{15}N^{14}N]$, where C_0 is the initial concentration of the deposit. Then Eq. [3] can be rearranged to

$$\partial[^{15}N^{14}N]/\partial t = k' \times (C_0 - [^{15}N^{14}N])^n. \quad [4]$$

Upon assuming $n = 1$ and integrating Eq. (4), we obtain

$$[^{15}N^{14}N] = C_0 \times (1 - e^{-k' \times t}). \quad [5]$$

That is the function observed experimentally for $^{15}N^{14}N$ formation in Fig. 1 and Table 1, which shows that the above assumptions are reasonable.

Since $k' = k \times P_{NO_2}^m$, it actually depends on the partial pressure of NO$_2$. The result in Fig. 2 shows that an equation $k' = k \times (b \times P_{NO_2}/(1 + b \times P_{NO_2})$ fits the experimental data well. This function indicates that the reaction rate can be formally described as a Langmuir–Hinshelwood mechanism. If impinging NO$_2$ molecules were to react directly with the deposit, a first-order dependence on P_{NO_2} would be expected. Figure 2 shows that no saturation is reached under the conditions used here, which is reasonable because $C_{Fe} \gg C_{deposit}$.

For a comparison of the deposits from different hydrocarbons, we thus can use k, or k', if comparison is limited to the same values of P_{NO_2}. Table 1 shows that the deposits formed with C_3H_8 and n-C_4H_{10} have similar reactivities, indicating that their chemical nature is probably similar. This is reasonable because both are straight chain alkanes. Whereas i-C_4H_{10} reacts more easily with NO$_y$ to form a deposit, as we reported previously (12), this deposit is less active in the following N$_2$ formation step than the deposits formed from the n-alkanes.

As to the model compounds, the k' values of NH$_3$ and $C_2H_5NH_2$ are very high, indicating a high reactivity toward NO$_2$. NH$_3$ has long been practically used as a reductant for the SCR of NO$_x$ from stationary sources (47). In this reaction, Fe/zeolite catalysts show high activity (48). Using $^{15}NH_3$ and ^{14}NO, over Cu/ZSM-5, Mizumoto *et al.* (49) showed that the formed N$_2$ is overwhelmingly $^{14}N^{15}N$. It is also well known that primary amines readily react with NO$_2$ forming diazo or diazonium compounds, which are fairly unstable and easily decompose to N$_2$.

Organic nitriles, cyanates, and/or isocyanates have been proposed as intermediates of SCR of NO$_x$ with hydrocarbons. Table 1 shows that CH$_3$CN over Fe/ZSM-5 does produce N$_2$ upon reacting with NO$_2$; however, its k' value is lower than those obtained over the real deposit laid down by the reaction of NO$_y$ with alkanes. Moreover, the FTIR results in Fig. 4 show that CH$_3$CN on Fe/ZSM-5 will

undergo hydrolysis, forming amide groups; these react more swiftly with NO_2. It thus seems that the first step for CH_3CN is hydrolysis, which is followed by reaction with NO_2. This is confirmed by the results shown in Fig. 5. Over H/ZSM-5, hydrolysis of CH_3CN is catalyzed by H^+; the amide groups formed readily react with NO_2. In contrast, over Na/ZSM-5, no hydrolysis of CH_3CN takes place and no N_2 was detected upon exposure to NO_2. Since adsorbed NH_3 on Na/ZSM-5 shows a reactivity comparable to that on Fe/ZSM-5, it follows that not the nitrile group but its hydrolysis product is responsible for the N_2 formation.

Although $CH_2{=}C(CH_3){-}CN$ also has a nitrile group, this deposit displays a lower k' value. Apparently, it is more stable against hydrolysis because the carbon–nitrogen triple bond is in resonance with the carbon–carbon double bond. This further confirms that the hydrolysis products, not the nitrile itself, react with NO_2. Interestingly, a considerable amount of $^{15}N_2$ was also observed in this case, in contrast to CH_3CN for which $^{15}N^{14}N$ is the only dinitrogen product. This indicates that the $C{=}C$ double bond is instrumental in the reduction of $^{15}NO_2$ and/or ^{15}NO molecules, a process which ultimately leads to $^{15}N_2$ formation. It has been found that NO reacts readily with olefines; in the presence of NO_2, dinitrogen is one of the products (50, 51).

Ethyl isocyanate is unstable over Fe/ZSM-5 at $200°C$. Figure 7 shows that it decomposes to isocyanate groups on the iron sites and unsaturated hydrocarbons that remain on the catalyst surface. Isocyanate groups are very reactive toward NO_2 as demonstrated by the high k' value in Table 1 and the spectrokinetic data in Fig. 7. Since unsaturated hyrocarbons are formed, a rather large amount of $^{15}N_2$ is detected in the gas phase.

The deposit formed by the decomposition of 2-nitropropane on Fe/ZSM-5 also reacts with $^{15}NO_2$, forming $^{15}N^{14}N$, though with a lower k' value. The FTIR spectra in Fig. 8 show $C{\equiv}N$ groups; also groups giving IR bands at 1670 and 1573 cm^{-1} might contain N. This result shows that organic nitro (or nitroso) compounds on the catalyst surface can undergo reactions, including isomerization, pyrolysis, and hydrolysis; eventually, an N-containing compound will be formed which can further react with NO_2, forming N_2.

The deposits formed by the reaction of NO_y with alkane or by decomposition of 2-nitropropane both show IR bands at 1670 and 1573 cm^{-1}; these bands decline quickly upon exposure to NO_2. On the basis of the spectra shown in Figs. 4 and 5 as well as the reactivity data toward NO_2, one can reasonably assume that these bands will contain a contribution from the amide(I) and amide(II) bands. To confirm this, we created an N-containing deposit over Fe/ZSM-5 by reaction of i-C_4H_{10} with NO_2 and measured the N1s binding energy by XPS. Peaks with a binding energy of 400.2 and 396.9 eV were observed. Upon comparison with literature data (52)

and also with the values measured with several reference compounds, the N1s peak at 396.9 eV can be assigned to a nitrile group, while the peak at 400.2 eV is assigned to an amide group. Interestingly, no N1s peak in a high oxidation state was observed.

Previously, it was shown that NO_y reacts with alkanes over Fe/ZSM-5, possibly via a free radical mechanism; organic nitro and/or nitroso compounds are the initial products (12). The N atom in these intermediates has a high oxidation state. Clearly, the primary products must undergo several reactions to become an active deposit with the N atom at a low oxidation state, such as an amine group. Such deposits can react with NO_2, forming a new nitrogen–nitrogen bond in an azo or diazo complex that will decompose by releasing N_2. The detailed reaction pathways for different alkanes will be addressed in a separate paper. The conclusion is that these valency lowering steps require the presence of an H atom in the α position with respect to the nitro (or nitroso) group. In the case of C_3H_8 or n-C_4H_{10}, α-H is available in the initial 2-nitro- (or nitroso-)propane (or butane); these intial products can, therefore, readily undergo further isomerization and hydrolysis reactions, such as oxime formation and Beckmann rearrangements. Eventually, a compound is formed with nitrogen at a low oxidation state, such as an amine or amide group. However, in the case of i-C_4H_{10}, the corresponding primary product, 2-nitro- (or nitroso-)2-methylpropane, does not have an α-H atom. Subsequent isomerizations will be more difficult for this hypothetical intermediate. We believe that this is the crucial cause for the lower reactivity of i-C_4H_{10} at low temperature as found experimentally; see Table 1.

5. CONCLUSIONS

Active intermediates can be formed on the Fe/ZSM-5 catalyst by reaction of adsorbed NO_y complexes with alkanes, including C_3H_8, n-C_4H_{10}, and i-C_4H_{10}. The reactivity of the intermediates at low temperature follows the sequence $C_3H_8 \approx n$-$C_4H_{10} > i$-C_4H_{10}. Mixed labeled $^{14}N^{15}N$ is the predominant N_2 product when the catalyst covered with a ^{14}N-containing deposit is exposed to $^{15}NO + O_2$. $^{15}N^{15}N$ will also be formed if unsaturated $C{=}C$ bonds are present in the deposit. A comparison with model compounds indicates that amino groups are the active N-containing groups that react with adsorbed nitrogen oxides. Nitriles first have to undergo hydrolysis, so that amine or amide groups are formed. As organic nitroso and/or nitro compounds are the most likely primary intermediates on the catalyst surface, chemical reactions are required to convert them to a deposit exposing amine or amide groups. These steps, in which the nitrogen valence is lowered, depend on the nature of the alkane; they are relatively easy if the primary intermediate contains an H atom in the α position with respect to the nitro (or nitroso) group.

REFERENCES

1. Iwamoto, M., and Mizuno, N., *Proc. Inst. Mech. Eng., Part D: J. Auto. Eng.* **207**, 23 (1992).
2. Shelef, M., *Chem. Rev.* **95**, 209 (1995).
3. Walker, A. P., *Catal. Today* **26**, 107 (1995).
4. Armor, J. N., *Catal. Today* **26**, 147 (1995).
5. Amiridis, M. D., Zhang, T., and Farrauto, R. J., *Appl. Catal. B* **10**, 203 (1996).
6. Gilot, P., Guyon, M., and Stanmore, B. R., *Fuel* **76**, 597 (1997).
7. Feng, X., and Hall, W. K., *Catal. Lett.* **41**, 45 (1996).
8. Feng, X., and Hall, W. K., *J. Catal.* **166**, 368 (1996).
9. Chen, H.-Y., and Sachtler, W. M. H., *Catal. Today* **42**, 73 (1998).
10. Chen, H.-Y., and Sachtler, W. M. H., *Catal. Lett.* **50**, 125 (1998).
11. Voskoboinikov, T., Chen, H.-Y., and Sachtler, W. M. H., *Appl. Catal. B* **19**, 279 (1998).
12. Chen, H.-Y., Voskoboinikov, T., and Sachtler, W. M. H., *J. Catal.* **180**, 171 (1998).
13. Ukisu, Y., Sato, S., Muramatu, G., and Yoshida, K., *Catal. Lett.* **11**, 177 (1991).
14. Ukisu, Y., Sato, S., Abe, A., and Yoshida, K., *Appl. Catal. B* **2**, 147 (1993).
15. Bell, B. A., Felley, J. S., Deeba, M., and Farrauto, R. J., *Catal. Lett.* **29**, 15 (1994).
16. Hayes, N. W., Grünert, W., Hutchings, G. J., Joyner, R. W., and Shpiro, E. S., *J. Chem. Soc., Chem. Commun.* 531 (1994).
17. Hayes, N. W., Joyner, R. W., and Shpiro, E. S., *Appl. Catal. B* **8**, 343 (1996).
18. Bethke, K. A., Li, C., Kung, M. C., Yang, B., and Kung, H. H., *Catal. Lett.* **31**, 287 (1995).
19. Li, C., Bethke, K. A., Kung, H. H., and Kung, M. C., *J. Chem. Soc., Chem. Commun.* 813 (1995).
20. Radtke, F., Koeppel, R. A., and Baiker, A., *Appl. Catal. A* **107**, L125 (1994).
21. Radtke, F., Koeppel, R. A., and Baiker, A., *Catal. Lett.* **28**, 131 (1994).
22. Radtke, F., Koeppel, R. A., and Baiker, A., *Catal. Today* **26**, 159 (1995).
23. Radtke, F., Koeppel, R. A., Minardi, E. G., and Baiker, A., *J. Catal.* **167**, 127 (1997).
24. Poignant, F., Saussey, J., Lavalley, J.-C., and Mabilon, G., *J. Chem. Soc., Chem. Commun.* 89 (1995).
25. Poignant, F., Saussey, J., Lavalley, J.-C., and Mabilon, G., *Catal. Today* **29**, 93 (1996).
26. Aylor, A. W., Lobree, L. J., Reimer, J. A., and Bell, A. T., *Stud. Surf. Sci. Catal.* **101**, 661 (1996).
27. Lobree, L. J., Aylor, A. W., Reimer, J. A., and Bell, A. T., *J. Catal.* **169**, 188 (1997).
28. Tanuka, T., Okuhara, T., and Misono, M., *Appl. Catal. B* **4**, L1 (1994).
29. Yokoyama, C., and Misono, M., *J. Catal.* **150**, 9 (1994).
30. Okuhara, T., Hasada, Y., and Misono, M., *Catal. Today* **35**, 83 (1997).
31. Li, Y., Slager, T. L., and Armor, J. N., *J. Catal.* **150**, 388 (1994).
32. Cant, N. W., Cowan, A. D., Doughty, A., and Haynes, B. S., *Catal. Lett.* **46**, 207 (1997).
33. Cowan, A. D., Cant, N. W., Haynes, B. S., and Nelson, P. F., *J. Catal.* **176**, 329 (1998).
34. Lombardo, E. A., Sill, G. A., d'Itri, J. L., and Hall, W. K., *J. Catal.* **173**, 444 (1998).
35. Blower, C. J., and Smith, T. D., *Zeolites* **13**, 394 (1993).
36. Yogo, K., Ono, T., Ogura, M., and Kikuchi, E., *in* "Reduction of Nitrogen Oxide Emission" (U. S. Ozkan, S. K. Agarwal, and G. Marcelin, Eds.), p. 123. ACS, Washington, DC, 1995.
37. Guyon, M., Le Chanu, V., Gilot, P., Kessler, H., and Prado, G., *Appl. Catal. B* **8**, 183 (1996).
38. Beutel, T., Adelman, B. J., Lei, G.-D., and Sachtler, W. M. H., *Catal. Lett.* **32**, 83 (1995).
39. Beutel, T., Adelman, B. J., and Sachtler, W. M. H., *Catal. Lett.* **37**, 125 (1996).
40. Adelman, B. J., Beutel, T., Lei, G.-D., and Sachtler, W. M. H., *Appl. Catal. B* **11**, L1 (1996).
41. Haber, F. Z., *Elektrochem.* 506 (1898).
42. March, J., "Advanced Organic Chemistry: Reactions, Mechanisms, and Structure," 2nd ed. McGraw-Hill, New York, 1977.
43. Socrates, G., "Infrared Characteristic Group Frequencies," 2nd ed. John Wiley & Sons, New York, 1994.
44. Unland, M. L., *J. Phys. Chem.* **77**, 1952 (1973).
45. Unland, M. L., *J. Catal.* **31**, 459 (1973).
46. Feuer, H. (Ed.), "The Chemistry of the Nitro and Nitroso Groups, Part I." Interscience Publishers, New York, 1969.
47. Bosch, H., and Janssen, F., *Catal. Today* **2**, 369 (1988).
48. Amiridis, M. D., Puglisi, F., Dumesic, J. A., Millman, W. S., and Topsøe, N.-Y., *J. Catal.* **142**, 572 (1993).
49. Mizumoto, M., Yamazoe, N., and Seiyama, T., *J. Catal.* **55**, 119 (1978).
50. Brown, J. F., *J. Am. Chem. Soc.* **79**, 2480 (1957).
51. Phillips, L. V., and Coyne, D. M., *J. Org. Chem.* **29**, 1937 (1964).
52. Moulder, J. F., Stickle, W. F., Sobol, P. E., and Bomben, K. D., *in* "Handbook of X-ray Photoelectron Spectroscopy" (J. Chastani, Ed.). Perkin-Elmer, Eden Prairie, MN, 1992.